PERGAMON

Phytochemistry 51 (1999) 223–236

PHYTOCHEMISTRY

Analysis of metabolic pathways via quantitative prediction of isotope labeling patterns: a retrobiosynthetic ^{13}C NMR study on the monoterpene loganin

Dietmar Eichinger[a], Adelbert Bacher[a], Meinhart H. Zenk[b], Wolfgang Eisenreich[a,*]

[a]*Lehrstuhl für Organische Chemie und Biochemie, Technische Universität München, Lichtenbergstraße 4, D-85747 Garching, Germany*
[b]*Institut für Pharmazeutische Biologie, Ludwigs-Maximilians-Universität München, Karlstr. 29, D-80333 München, Germany*

Received 6 October 1998

Abstract

The monoterpene loganin serves as a precursor in the biosynthetic pathways of numerous indole alkaloids. In contrast to earlier studies, we present evidence that the biosynthesis of loganin in *Rauwolfia serpentina* cells proceeds mainly via the deoxyxylulose pathway and not by the mevalonate pathway. This conclusion is based on experiments using a *R. serpentina* cell culture supplied with ^{13}C-labeled samples of glucose, ribose/ribulose, pyruvate or glycerol. Loganin was isolated from biomass, and the hydrolysis of cellular protein afforded amino acids. The isolated metabolites were analyzed by NMR spectroscopy. The ^{13}C-labeling patterns of isolated amino acids were then used to reconstruct the labeling patterns of phosphoenol pyruvate, pyruvate and acetyl CoA. These labeling patterns were subsequently used to predict labeling patterns for dimethylallyl pyrophosphate and isopentenyl pyrophosphate via the mevalonate and deoxyxylulose pathway, respectively. The observed labeling patterns of the terpenoid moieties in loganin were in excellent agreement with the deoxyxylulose prediction. The minor incorporation of mevalonate into loganin observed in earlier studies can be attributed to metabolite exchange between the two terpenoid pathways. The possibility of crosstalk between the two pathways in plants and plant cell cultures stresses the need for a quantitative analysis of general carbon metabolism in order to determine the partitioning between the mevalonate and deoxyxylulose pathway. The present study shows that a wide variety of general metabolic precursors can fulfill this task in conjunction with the retrobiosynthetic concept.

Keywords: *Rauwolfia serpentina*; Apocynaceae; Loganin; Isoprenoid biosynthesis; Deoxyxylulose pathway; Indole alkaloids; NMR; Retrobiosynthesis

1. Introduction

The ring system of loganin (**9**, Fig. 1) is assembled from one molecule each of the universal terpenoid precursors dimethylallyl pyrophosphate (**1**) (DMAPP) and isopentenyl pyrophosphate (**2**, IPP) via geranyl pyrophosphate (**3**). Cyclization of the intermediate (**4**) yields the cyclopentane derivative (**5**) which is then further elaborated via (**8**) to the final compound (**9**) (for review see Banthorpe, Charlwood, & Francis, 1972; Uesato, Kanomi, Iida, Inouye, & Zenk, 1986).

Pioneering studies by Bloch, Cornforth, Lynen and their coworkers had shown that IPP (**2**) can be formed from three molecules of acetyl CoA (**10**) via mevalonate (**11**) in yeast and animal cells (Fig. 2; for review see Qureshi & Porter, 1981; Bloch, 1992). DMAPP (**1**) was shown to be formed from IPP by a reversible isomerization step (for review see Ramos-Valdivia, van der Heijden, & Verpoorte, 1997).

During a period of several decades, the mevalonate pathway was considered as the unique biosynthetic route to terpenoids, although numerous experimental observations obtained with plants and certain bacteria

* Corresponding author. Tel.: +49-89-289-13043; fax +49-89-289-13363.
E-mail address: wolfgang.eisenreich@ch.sum.de (W. Eisenreich)

0031-9422/99/$ - see front matter
PII: S0031-9422(98)00733-X

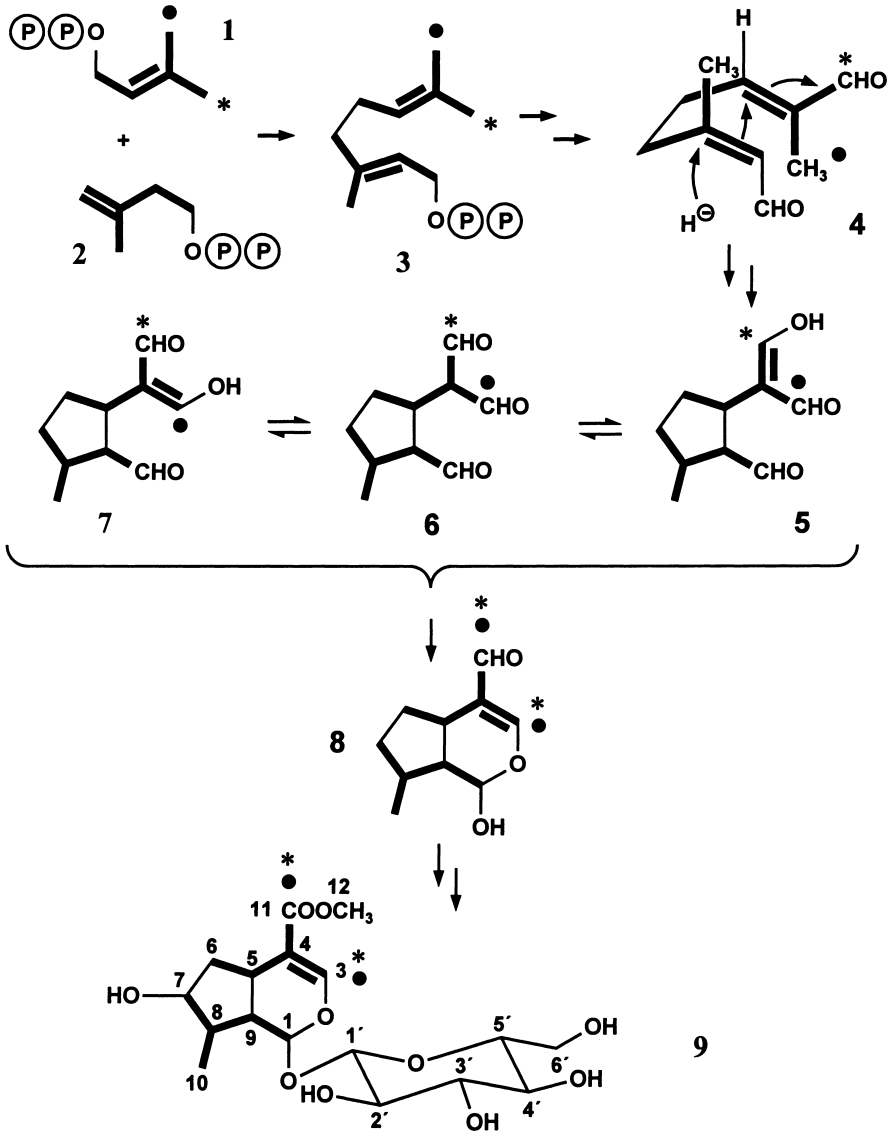

Fig. 1. Pathway which has been proposed in the literature for the biosynthesis of loganin (for review, see Banthorpe et al., 1972; Stöckigt, 1979). The isoprene dissection of the monoterpene is indicated by bold bars.

were not easily explained. An alternative terpenoid pathway operative in plants and certain microorganisms was detected relatively recently by independent contributions from Rohmer, Arigoni, Sahm and their research groups (Fig. 2; for review see Eisenreich et al., 1998; Rohmer, 1998). More specifically, Rohmer, Sahm and their coworkers showed that the transformation of ^{13}C-labeled glucose and acetate into bacterial hopanoids could not be explained by the classical mevalonate hypothesis (Flesch & Rohmer, 1988; Rohmer, Knani, Simonin, Sutter, & Sahm, 1993). Independently, Arigoni and his coworkers (Schwarz, 1994) using uniformly ^{13}C-labeled glucose as precursor had shown that the biosynthesis of ginkgolides by seedlings of *Ginkgo biloba* involves the incorporation of a three-carbon fragment, whereas only two-carbon moieties are involved in the mevalonate pathway. Using various ^{13}C labeled glucose samples, Arigoni and his coworkers were also able to show that the formation of ubiquinone in *Escherichia coli* proceeds via the non-mevalonate pathway (Broers, 1994).

The enzyme catalyzing the formation of 1-deoxy-D-xylulose 5-phosphate (**14**) from glyceraldehyde 3-phosphate (**13**) and pyruvate (**12**) in the alternative pathway has been described from *E. coli* (Sprenger et al., 1997; Campos, Lois, & Boronat, 1997; Lois et al., 1998) and from *Mentha piperita* (Lange, Wildung, McCaskill, & Croteau, 1998). The further conversion of 1-deoxy-D-xylulose 5-phosphate (**14**) to 2-*C*-methyl-D-erythritol 4-phosphate (**15**) was recently demonstrated to proceed in a single step by intramolecular rearrangement and reduction via an enzyme which was cloned and

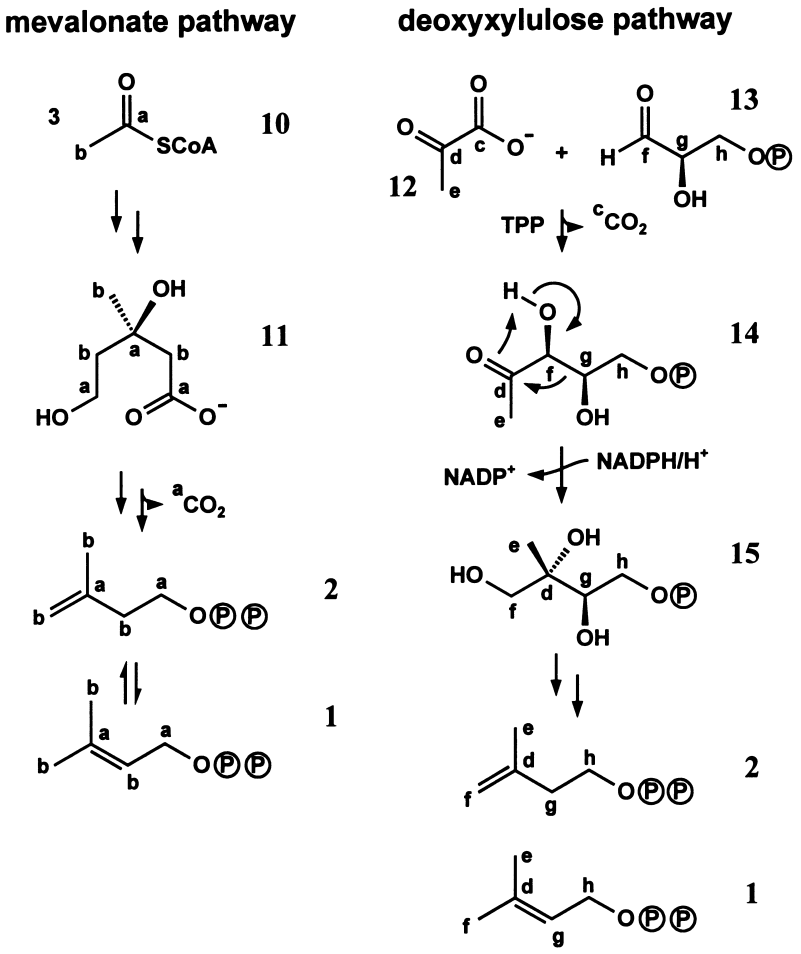

Fig. 2. Diversion of carbon atoms from precursors to isoprenoid monomers by the mevalonate pathway (precursor, acetyl CoA) and the deoxyxylulose pathway (precursors pyruvate and glyceraldehyde 3-phosphate). The deoxyxylulose pathway involves a rearrangement of 1-deoxy-D-xylulose 5-phosphate which interrupts the contiguity of the carbon atoms derived from the triose phosphate precursor.

expressed from *E. coli* (Takahashi, Kuzuyama, Watanabe, & Seto, 1998).

Both terpenoid pathways have been shown to occur in cells of higher plants (for review see Eisenreich et al., 1998; Rohmer, 1998). Specifically, the mevalonate pathway appears to be operative in the cytoplasmic compartment where it is supplying the building blocks for the biosynthesis of sterols. The deoxyxylulose pathway (Fig. 2) appears to be compartmentalized in plastids and has been shown to yield phytol as well as a variety of hemiterpenes, monoterpenes, diterpenes and carotenoids (Arigoni et al., 1997; Schwender et al., 1997).

The biosynthetic origin of DMAPP and IPP used for the biosynthesis of loganin had been investigated repeatedly using ^{14}C- and ^{3}H-labeled mevalonate as precursors. Incorporation of radioactivity from mevalonate into the terpenoid moiety of loganin from *Vinca rosea* was documented unequivocally, however in low rates (Battersby et al., 1968; Escher, Loew, & Arigoni, 1970; Guarnaccia, Botta, & Coscia, 1974). On the other hand, no incorporation from radiolabeled mevalonate into loganin was observed using other *Vinca* species (D. Arigoni, personal communication). Similarly, ^{14}C-mevalonate was not significantly incorporated into loganin from *Menyanthes trifoliata*, but was efficiently used as a precursor for triterpenes and sterols in the same biological system (Brechbühler-Bader, Coscia, Loew, Sczepanski, & Arigoni, 1968). Despite those conflicting results, it was widely assumed until recently that loganin is derived from mevalonate (Verpoorte, van der Heijden, & Moreno, 1997; Whitmer, Canel, Hallard, Gonçalves, & Verpoorte, 1998; Shanks, Bhadra, Morgan, & Rijhwani, 1998).

In light of the important role of loganin as a precursor of over 2000 indole alkaloids known to date, we decided to investigate its biosynthetic origin by retrobiosynthetic analysis which permits the quantitative analysis of metabolite flux patterns. This method uses information gleaned from isotope distribution patterns in primary metabolites in order to interpret the labeling patterns of secondary metabolites.

The data show that the bulk of loganin (>95%) in *R. serpentina* is formed via the deoxyxylulose pathway. The earlier studies with radioisotopes have apparently detected a minor contribution from the mevalonate pathway to the two C_5 building blocks from which loganin is assembled.

2. Results

2.1. Experimental strategy

The products of secondary metabolism are derived from amino acids or from central metabolic intermediates (e.g. of the Embden–Meyerhof pathway, the pentose phosphate cycle and the citrate cycle). In isotope labeling experiments, the labeling pattern of each metabolite studied must therefore reflect the labeling patterns of the precursor molecules from which it has been assembled in the biosynthetic process.

The retrobiosynthetic method described in the following section utilizes general metabolic precursors such as carbohydrates, polyols and carboxylic acids as isotope-labeled tracers. These general metabolites can divert isotopic label to virtually all branches of cellular metabolism. The metabolites generated in these experiments are complex isotopomer mixtures, since the label of the proffered precursor can be reshuffled extensively during its passage through linear and/or cyclic pathways of intermediary metabolism (Werner, Bacher, & Eisenreich, 1997).

Amino acids can be easily isolated after hydrolytic treatment of isotope-labeled biomass. Their isotopomer compositions can be determined quantitatively by one- and two-dimensional NMR analysis when ^{13}C, ^{15}N, ^{2}H or any combination of these isotopes are used as labels in the proffered precursor. On basis of known biosynthetic pathways, these data can then be used to reconstruct the labeling patterns of central intermediary metabolites.

If a given metabolite can be biosynthesized alternatively via different biosynthetic pathways, the labeling pattern for each respective pathway can be predicted quantitatively using the experimentally determined labeling patterns of central, primary intermediates. These predicted labeling patterns can then be compared with the observed labeling pattern of the secondary metabolite under study. Metabolic pathways which predict labeling patterns at odds with the observed pattern can be ruled out with a high degree of certainty. In cases where a given metabolite can be formed simultaneously via more than one metabolic pathway, the partitioning of metabolite flux through the different pathways can be estimated (for review see Bacher et al., 1998). The application of this general method to the biosynthesis of loganin in *R. serpentina* cell cultures is described in detail below.

2.2. Isotope incorporation studies

Cell cultures of *R. serpentina* were grown with D-glucose as carbon source. The time for doubling of cell mass was 18 days. Isotope labeled precursors were added as a bolus at the beginning of the growth phase (Table 1). After two weeks of growth, the cells were harvested, and loganin was isolated as described in Section 4. Typically, 45 mg of the monoterpene were obtained from 100 g of wet cell mass. The remaining cell mass was subsequently hydrolyzed to yield amino acids. The ^{13}C labeling patterns of biosynthetic loganin and selected amino acids were assessed quantitatively by one- and two-dimensional NMR analysis (Table 2).

2.3. Labeling patterns of central intermediates

In order to predict the labeling pattern of DMAPP/IPP via the mevalonate and the deoxyxylulose pathway Fig. 2, the labeling patterns of the specific precursors for each of these pathways are required. Specifically, acetyl CoA is the unique precursor of the mevalonate pathway; glyceraldehyde 3-phosphate and pyruvate act as precursors of 1-deoxy-D-xylulose 5-phosphate in the alternative pathway.

The carboxylic group and the α carbon of leucine (**16**) are derived from acetyl CoA (**3**) via condensation

Table 1
Isotope incorporation experiments with cell cultures of *Rauwolfia serpentina*. The precursors were added as a bolus at the beginning of the growth phase

Precursor	Concentration (mM)	Unlabeled glucose (mM)	Culture volume (ml)
[U–$^{13}C_6$]glucose	6.4	160.0	750
[1–^{13}C]glucose	165.7	0	100
[2–^{13}C]glucose	82.9	83.3	30
[3–^{13}C]glucose	165.7	0	17
[U–$^{13}C_5$]ribulose/ribose	2.1/1.0	166.7	600
[3–^{13}C]sodium pyruvate	29.7	83.3	300
[2–^{13}C]glycerol	43.0	72.2	250

Table 2
^{13}C labeling patterns of loganin from cell cultures of *Rauwolfia serpentina* grown with ^{13}C-labeled glucoses, pyruvate, glycerol or ribulose/ribose

Position	^{13}C-Abundances and $^{13}C^{13}C$ couplings								
	[U–$^{13}C_6$]glucose		[1-^{13}C]-glucose	[2-^{13}C]-glucose	[3-^{13}C]-glucose	[U–$^{13}C_5$]ribulose/ribose		[3-^{13}C]-pyruvate	[2-^{13}C]-glycerol
	% $^{13}C^a$	% $^{13}C^{13}C^b$	% $^{13}C^a$	% $^{13}C^a$	% $^{13}C^a$	% $^{13}C^a$	% $^{13}C^{13}C^b$	% $^{13}C^a$	% $^{13}C^a$
1	3.5	60.9(9), 36.1(7)	28.4	4.1	4.5	2.3	39.2(9), 21.1(7)	1.9	3.0
9	3.4	61.6(1)	2.3	12.1	10.8	2.3	39.7(1)	1.8	16.0
8	3.5	56.2(10)	7.0	11.7	9.3	2.2	30.0(10), 5.0(7)	2.8	17.3
10	3.2	56.6(8)	30.5	4.1	4.7	2.1	31.5(8)	6.0	3.1
7	3.4	5.6(8)	4.8	4.0	32.8	2.3	5.9(8)	1.7	2.9
6	3.3	58.7(5)	28.5	4.2	5.4	2.3	38.9(5)	1.9	3.5
5	3.1	63.0(6)	2.6	11.9	10.5	2.3	39.9(6)	1.8	16.2
4	3.5	25.4(3), 28.0(11)	6.3	12.5	7.3	2.1	15.4(3), 15.2(11)	2.7	17.4
11	3.4	29.0(4)	17.9	3.8	17.6	2.2	15.4(4)	3.7	3.0
3	3.3	30.2(4)	18.4	3.8	18.4	2.1	16.0(4)	4.0	3.1
1′	3.4	65.3(2′)	52.6	3.6	4.4	1.9	20.3(2′), 6.3(3′)	1.9	2.8
2′	3.7	45.8(1′ and 3′), 21.5(1′)	2.2	21.6	9.5	1.8	21.7(1′), 8.5(1′ + 3′)	1.8	12.5
3′	3.8	32.7(2′ and 4′), 27.9(2′ or 4′)	3.9	4.1	68.9	2.1	7.5(2′), 10.4(4′)	1.6	2.2
4′	3.8	31.3(3′ and 5′), 34.0(3′ or 5′)	3.2	2.8	26.3	2.0	10.0(3′), 15.7(5′)	1.6	2.3
5′	3.4	49.6(4′ and 6′), 19.0(6′)	2.0	9.8	7.2	1.8	16.2(6′), 15.2(4′ + 6′)	1.8	12.8
6′	3.5	66.0(5′)	24.1	3.1	3.6	1.8	30.9(5′)	1.8	2.5
12	3.6		21.4	5.0	4.9	2.2		2.8	6.6

[a] Absolute ^{13}C abundance.
[b] Percent coupling calculated as percentage of total signal for a given carbon atom involved in $^{13}C^{13}C$ coupling. Carbons coupled to the respective index carbon are in parentheses.

with α-ketoisovalerate. The labeling pattern of C-1 and C-2 of the leucine therefore reveals the labeling pattern of acetyl CoA (Fig. 3). Alanine (**17**) is biosynthetically obtained by reductive amination of pyruvate (**12**). Hence, the labeling pattern of pyruvate in each respective experiment can be gleaned from that of alanine isolated from cell protein Fig. 3. The side chains of phenylalanine (**18**) and tyrosine (**19**) are derived from phosphoenol pyruvate (**20**) via chorismic acid. Hence, the labeling patterns of the aromatic amino

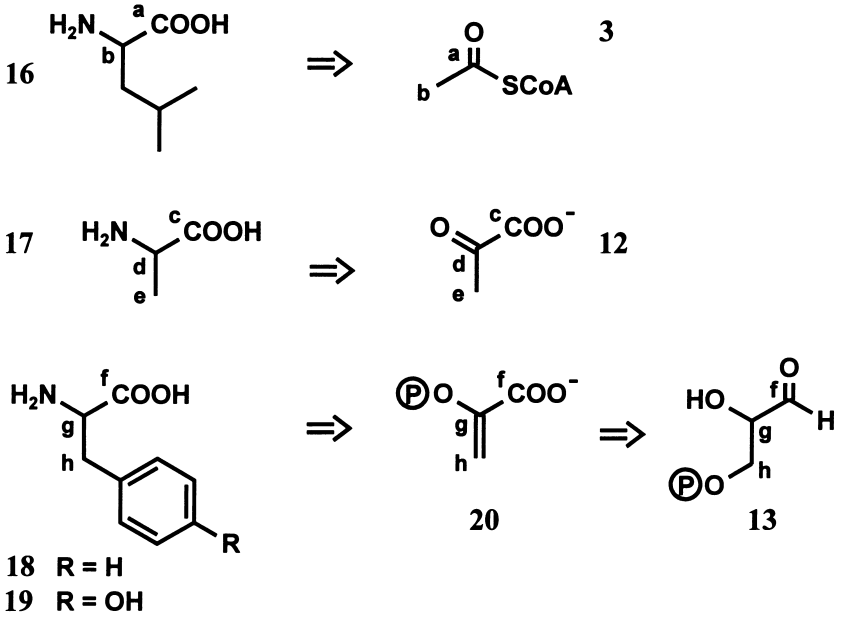

Fig. 3. Retrobiosynthetic analysis of amino acids, synthesized from central metabolic intermediates. Reconstruction of central labeling patterns is indicated by the symbol ⇒.

Table 3
^{13}C isotopomer composition of acetyl CoA, pyruvate and phosphoenol pyruvate in *Rauwolfia serpentina* after labeling with ^{13}C glucoses, pyruvate, glycerol and ribulose/ribose

Isotopomer	Abundance (mol %)						
	[U–$^{13}C_6$]glucose	[1-^{13}C]glucose	[2-^{13}C]glucose	[3-^{13}C]glucose	[3-^{13}C]pyruvate	[2-^{13}C]glycerol	[U-$^{13}C_5$]ribulose/ribose
Acetyl CoA							
[1-^{13}C]	1.1	3.9	12.0	9.8	2.2	17.2	1.5
[2-^{13}C]	1.5	25.5	3.1	5.8	15.5	3.1	1.3
[1,2-$^{13}C_2$]	1.2						0.5
Pyruvate							
[1-^{13}C]	1.9	4.5	6.9	31.5	2.0	4.8	1.8
[2-^{13}C]	1.2	5.2	11.5	5.6	1.3	17.7	1.5
[3-^{13}C]	1.3	31.1	4.1	3.5	6.8	4.0	1.6
[1,2-$^{13}C_2$]	0.1						0.1
[2,3-$^{13}C_2$]	0.7						0.3
[1,2,3-$^{13}C_3$]	1.1						0.3
Phosphoenol pyruvate							
[1-^{13}C]	2.6	3.6	3.1	ND[a]	1.3	2.5	1.4
[2-^{13}C]	1.3	2.6	12.8	ND[a]	2.2	15.9	1.5
[3-^{13}C]	1.4	28.9	3.0	ND[a]	2.2	3.2	1.7
[1,2-$^{13}C_2$]	0.1						0.1
[2,3-$^{13}C_2$]	0.8						0.4
[1,2,3-$^{13}C_3$]	1.4						0.3

[a] ND means not determined.

acid side chains must reflect that of phosphoenol pyruvate (Fig. 3).

Reconstructed isotopomer compositions for acetyl CoA, pyruvate and phosphoenol pyruvate from experiments using ^{13}C labeled specimens of glucose, ribulose/ribose, pyruvate and glycerol are summarized in Table 3. Even in the experiments with single labeled precursors, the acetyl CoA, pyruvate and phosphoenol pyruvate pool consisted of a complex mixtures of isotopomers. This is easily explained because the general precursors used in this study can be recycled in the central compartments of intermediary metabolism.

Similarly, the multiply labeled precursors [U–$^{13}C_6$]glucose and [U–$^{13}C_5$]ribulose/-ribose afforded complex isotopomer mixtures including various multiply labeled molecular species. Universally ^{13}C labeled C_2- and C_3-fragments can be generated metabolically from the breakdown of totally labeled precursors and can be diverted to downstream metabolites. On the other hand, the recycling of universally labeled fragments through central metabolic pathways can result in breaking of CC bonds. Subsequently, the resulting fragments can be used for the regeneration of metabolites such as pyruvate and phosphoenol pyruvate. This will usually involve the recombination of fragments from both labeled and unlabeled precursor molecules, and this explains the formation of single-labeled and double-labeled as well as triple-labeled pyruvate and phosphoenol pyruvate from totally labeled precursors (Table 3).

2.4. Labeling patterns of loganin

The mevalonate pathway implies the formation of IPP from three acetate moieties (Fig. 2). On basis of the reconstructed acetyl CoA labeling patterns (Table 3), the hypothetical labeling pattern of IPP via the mevalonate pathway can be predicted quantitatively, as shown in Fig. 4c for the experiment with the mixture of [U–$^{13}C_6$]glucose and unlabeled glucose. Specifically, the reconstructed pattern of acetyl CoA is characterized by a significant contribution from a doubly ^{13}C labeled isotopomer. Following the mevalonate pathway, contiguously ^{13}C labeled atoms would then be present in C1/C2 and C3/C5 of IPP and DMAPP (Fig. 4c).

The formation of the loganin ring system has been studied in considerable detail (for review see Banthorpe et al., 1972; Stöckigt, 1979). The committed precursor, geranyl pyrophosphate, biosynthesized from one molecule each of IPP and DMAPP, is converted via cyclization and oxidation of the intermediate (**4**) (Fig. 1) into the cyclopentane intermediate (**5**) which is in rapid equilibrium with its tautomeric form (**7**) via (**6**). As a consequence, the terminal enolic carbon of (**5**) as well as that of (**7**) (labeled with • and * in Fig. 1) participate in the bond making process yielding the

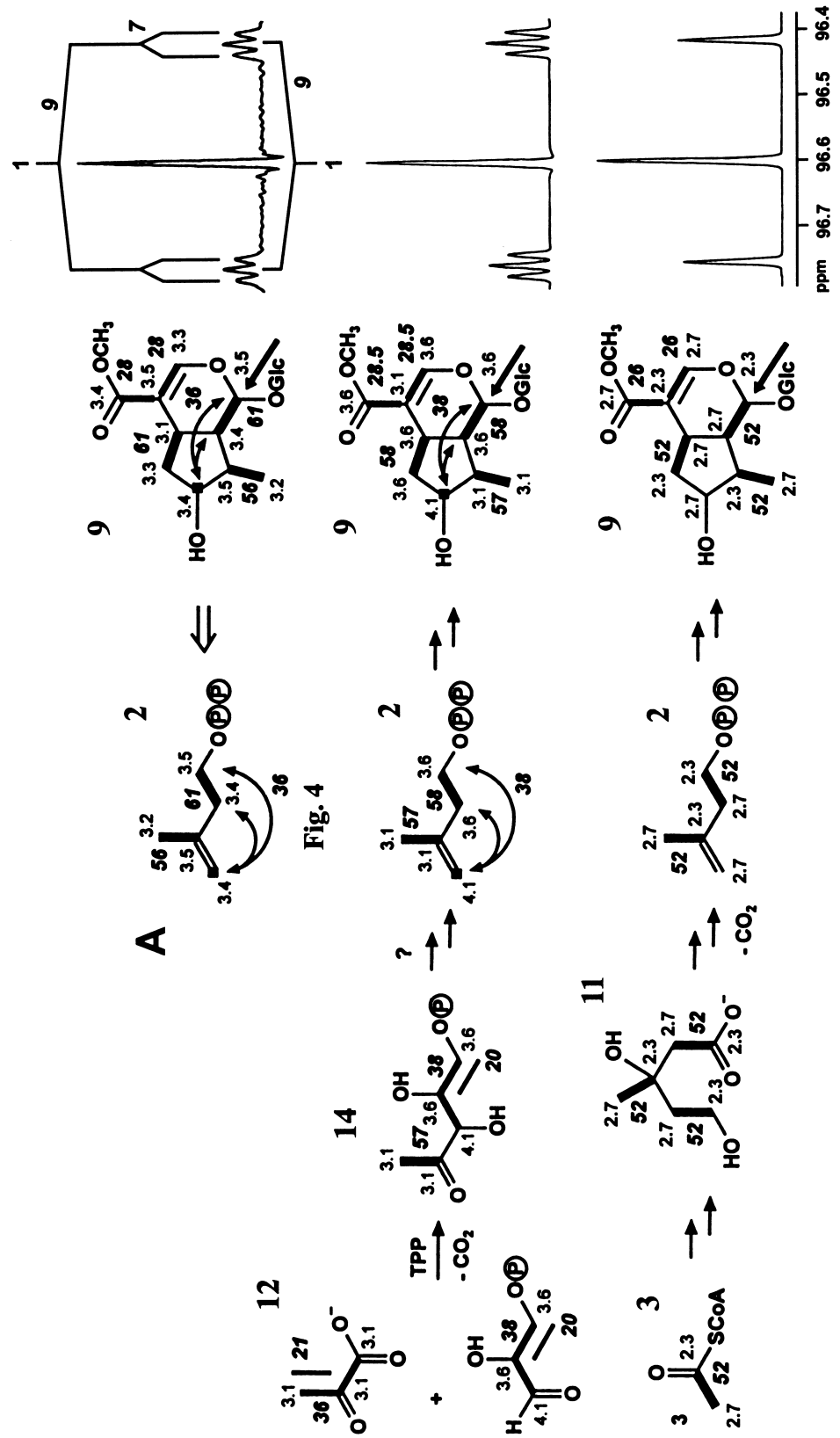

Fig. 4. Observed and predicted labeling patterns for loganin and the ^{13}C NMR signal of C-1 (indicated by an arrow) after feeding [U–$^{13}C_6$]glucose diluted with unlabeled glucose (1:24; w/w) to cell cultures of *Rauwolfia serpentina*. (a) observed; the isotopomer pattern of IPP was reconstructed from the observed labeling pattern in loganin. (b) prediction via the deoxyxylulose pathway; (c) prediction via the mevalonate pathway.

hemiacetal ring system in (**8**) (Escher et al., 1970). Thus, the original methyl groups of the DMAPP unit become randomized with respect to their label distribution. In other words, the carbon atoms 3 and 11 of loganin (Fig. 1) become indistinguishable with respect to their ^{13}C-abundance. On basis of these established mechanisms, IPP contributes the carbon atoms 1, 7, 8, 9 and 10 of loganin, and DMAPP contributes the loganin carbons 3, 4, 5, 6 and 11 of loganin (**9**, Fig. 1). Following this dissection the labeling patterns of loganin are now predicted from the labeling patterns of the C_5 building blocks as shown for the experiment with [U–$^{13}C_6$]glucose in Fig. 4c. The hypothetical labeling pattern of loganin biosynthesized via the mevalonate pathway is then characterized by blocks of ^{13}C atoms including the carbon pairs C1/C9, C8/C10, C5/C6, C3/C4, and C4/C11 (shown by bold lines in Fig. 4c). Using this isotopomer pattern, hypothetical ^{13}C NMR signals of loganin can now be simulated. For an example, the ^{13}C NMR signal of C-1 of loganin (indicated by an arrow in Fig. 4) biosynthesized via mevalonate would reflect a [1-$^{13}C_1$]- and a [1,9-$^{13}C_2$]-isotopomer resulting in a singlet and a doublet substructure of the ^{13}C NMR signal, respectively (Fig. 4c).

This experimental approach is now used for a quantitative prediction of the isotopomer pattern of loganin biosynthesized via the deoxyxylulose pathway. A central intermediate in the novel terpenoid pathway is 1-deoxy-D-xylulose 5-phosphate (**14**) which is assembled from glyceraldehyde 3-phosphate (**13**) and pyruvate (**12**) (Fig. 2). The labeling pattern of glyceraldehyde 3-phosphate is not directly represented in the proteolytic amino acids. However, since phosphoenol pyruvate is obtained from glyceraldehyde 3-phosphate (**13**) by dehydrogenation, isomerization and dehydration, its labeling pattern can serve as a substitute for the elusive glyceraldehyde pattern (Fig. 3). The hypothetical labeling pattern of IPP formed via the deoxyxylulose pathway is therefore reconstructed from the labeling patterns of pyruvate and glyceraldehyde 3-phosphate. Specifically, a significant contribution from [1,2,3-$^{13}C_3$]glyceraldehyde 3-phosphate is expected in the isotopomer pattern of compound **14** yielding [3,4,5-$^{13}C_3$]1-deoxy-D-xylulose 5-phosphate. Due to the rearrangement process yielding 2-*C*-methyl-D-erythritol 4-phosphate (**15**) (Fig. 2) the formation of [1,2,4-$^{13}C_3$]IPP would result, which is subsequently converted into [1,7,9-$^{13}C_3$]loganin.

As described above, hypothetical ^{13}C NMR signals are now simulated from the predicted labeling patterns (Fig. 4b). Most notably, the [1,7,9-$^{13}C_3$]loganin isotopomer in loganin causes the appearance of a double doublet substructure in the ^{13}C NMR signal of C-1 reflecting simultaneous ^{13}C coupling to C-9 ($^1J_{CC}$ = 43.5 Hz) and C-7 ($^3J_{CC}$ = 4.15 Hz).

As shown in Fig. 4, the observed labeling patterns of loganin and its IPP building block, as well as the observed ^{13}C NMR signal of C-1 is in almost perfect agreement to the predictions via the deoxyxylulose pathway.

Starting from various ^{13}C-labeled samples of glucose, ribose/ribulose, pyruvate or glycerol and using the retrobiosynthetic concept described above in detail the predicted labeling patterns of IPP formed via the deoxyxylulose pathway are in close agreement with the experimentally determined IPP labeling patterns in loganin (Fig. 5). On the other hand, the predictions via the mevalonate pathway are clearly at odds with the observed labeling patterns. It follows that, if not completely, at least the major fraction of loganin (>95%) has been obtained via the deoxyxylulose pathway in the experimental system used.

Since loganin is undoubtedly the precursor of secologanin (Battersby, Burnett, & Parsons, 1969; Tanahashi, Nagakura, Inouye, & Zenk, 1984) one can assume that all monoterpenoid indole alkaloids as well as the dopamine derived isoquinoline alkaloids of the emetine type are biosynthesized via condensation of pyruvate and glyceraldehyde-3-phosphate.

3. Discussion

Recent studies show that the universal terpenoid precursors, IPP and DMAPP, can be biosynthesized via two different pathways in higher plants. There is indirect evidence that the mevalonate pathway is operative in the cytoplasm, and the deoxyxylulose pathway is operative in plastids. However, the compartmental separation of the two pathways is not absolute. Exchange of metabolites between the two pathways occurs to a variable degree in different experimental systems (Arigoni et al., 1997). The crosstalk between the two pathways is not understood in detail. The specific metabolite or metabolites involved in the supposed intercompartmental exchange process are unknown.

In light of these recent findings, it is easily understood that earlier studies documented the incorporation of mevalonate into virtually all plant terpenoids studied. The low incorporation rates of mevalonate observed in many experiments were explained by poor uptake of the isotope-labeled precursor and compartmentalization of metabolic pathways. Direct experiments to determine the uptake rate were not performed and, indeed, would have been difficult to perform with sufficient accuracy. In retrospect, it appears that in many cases the observed incorporation of mevalonate were due to the crosstalk between the pathways and did not reflect the mainstream metabolite flux.

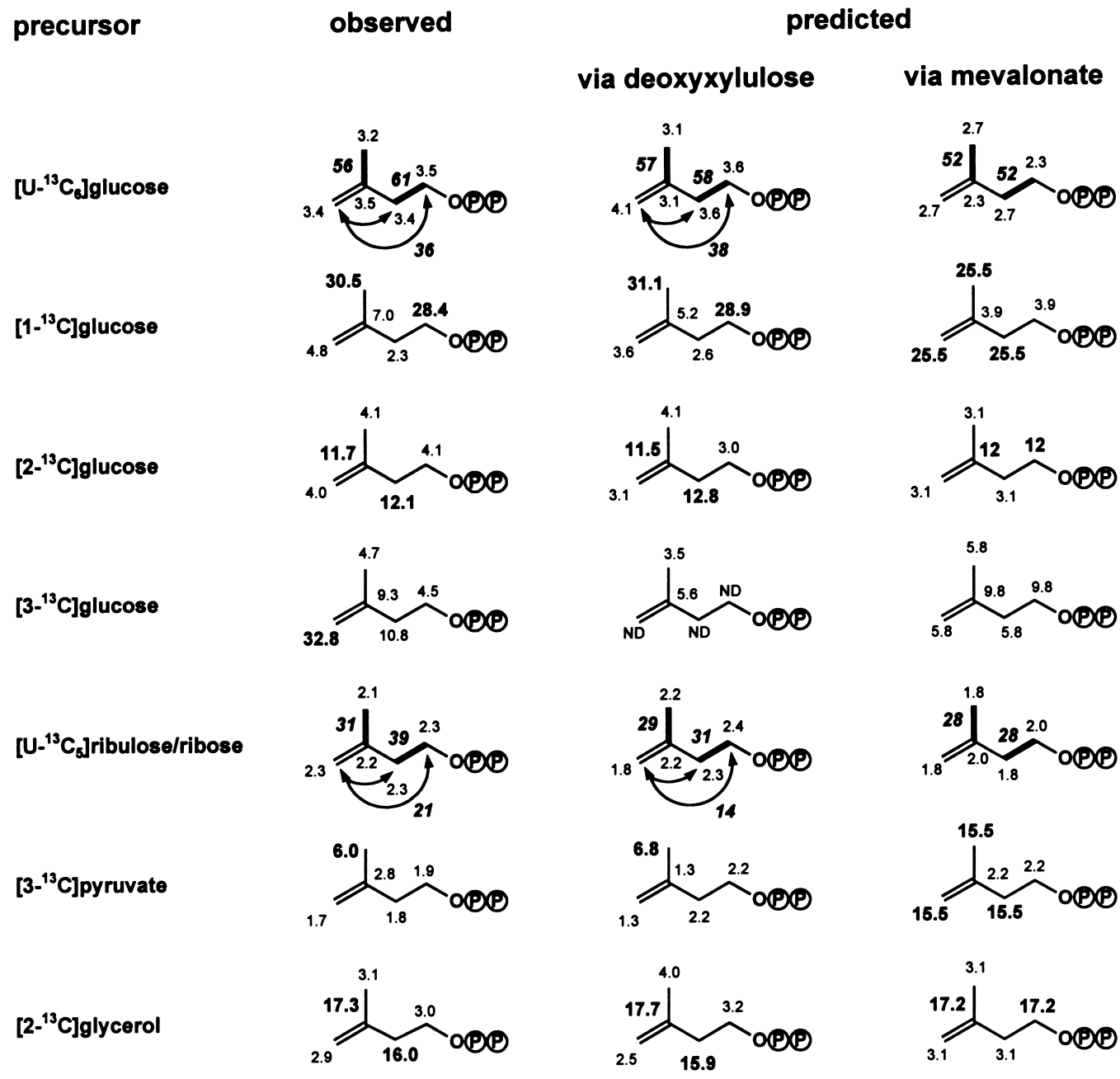

Fig. 5. Observed and predicted isotopomer patterns of the IPP moiety in loganin after growing cell cultures of *Rauwolfia serpentina* with various stable isotope labeled precursors. Predictions of the IPP labeling pattern were made on basis of the labeling data of pyruvate and phosphoenol pyruvate (deoxyxylulose pathway) or acetate (mevalonate pathway), as reconstructed from amino acids.

In recent studies, isotope-labeled 1-deoxy-D-xylulose has been used as a precursor to study the biosynthetic origin of terpenoids. These studies are faced with similar problems as the older work with mevalonate. The uptake of deoxyxylulose into the cell compartments involved in the biosynthesis of a specific terpenoid is unpredictable. For example, the carbohydrate is efficiently utilized for biosynthesis of ubiquinones in *E. coli* (Broers, 1994), of 2-*C*-methyl-D-erythritol in leaves of *Liriodendron tulipifera* (Sagner et al., 1998), and of carotenoids in cell cultures of *Catharanthus roseus* (Arigoni et al., 1997). On the other hand, 1-deoxy-D-xylulose was not significantly incorporated into taxoids in cells of *Taxus chinensis* (Menhard, 1998) and in cultures of *Methylobacterium organophilum*, *Corynebacterium ammoniagenes* (T. Duvold, P. Cali and M. Rohmer, unpublished work, quoted in Disch, Schwender, Müller, Lichtenhaler, &

Rohmer, 1998) and *Ochromonas danica* (C. Müller and H.K. Lichtenthaler, unpublished work, quoted in Disch et al., 1998) although it has been shown by other experiments that the terpenoids under study were assembled predominantly from isoprenoid precursors derived from the deoxyxylulose pathway. Thus, 1-deoxy-D-xylulose and mevalonate may not be suitable as exogenous precursor for labeling experiments in order to examine the partitioning between the two terpenoid pathways in plants and plant cell cultures.

The retrobiosynthetic concept described in this article is a universal method for analysis of metabolite flux. Any labeled compounds which can be diverted to all major areas of cellular metabolism can be used as precursor for this method. The labeling patterns of primary metabolites (amino acids, nucleosides) are determined and are used to reconstruct the isotopomer patterns of central metabolites on basis of known biosynthetic pathways. These procedures have been reviewed recently (Bacher et al., 1998) and are therefore not described in detail.

In order to assess the flux contributions of different pathways for the formation of given compounds which can be obtained via more than one route, the isotopomer pattern is predicted quantitatively for each of the possible pathways from the labeling patterns of the central metabolites (Fig. 5). The predicted isotopomer patterns are then compared to the experimentally determined label distribution in the metabolite under study. In the present case, the labeling patterns of loganin are in excellent agreement with the deoxyxylulose prediction (Fig. 5). This shows that the bulk amount of loganin is biosynthesized via the deoxyxylulose pathway.

Earlier reports suggesting the incorporation of mevalonate into loganin in low yields (Battersby et al., 1968; Escher et al., 1970; Guarnaccia et al., 1974) remain valid, even in light of the data reported in this paper, but they need to be reinterpreted. The low incorporation rate found in the old experiments were not (or at least not exclusively) a consequence of poor metabolite uptake. Instead, they represent a small amount of loganin formed from precursors contributed via the mevalonate pathway via crosstalk between the pathways.

In principle, each of the seven incorporation experiments in the present study would have been sufficient to prove that the formation of loganin in *R. serpentina* cells occurs predominantly via the deoxyxylulose branch of terpenoid metabolism. The parallel experiments with different metabolites and/or label positions in a given precursor were performed to check the general validity of the retrobiosynthetic concept. Indeed, the data show that each of the precursor species used yields the same conclusion (Fig. 5). The close agreement between the experiments actually suggests that every labeling strategy conducive to the diversion of label to all metabolic branches, but not to a rigorously stochastic label distribution (equivalent to a maximum of the isotopomer entropy term) can be used for the analysis of metabolic partitioning based on analysis of isotopomer patterns. Thus, precursors can be selected on basis of price, availability and efficiency of metabolic utilization rather than of their specific metabolic proximity to the intermediate of the respective pathway.

4. Experimental

4.1. Chemicals

[U–$^{13}C_6$]-, [1-^{13}C]-, [2-^{13}C]-, [3-^{13}C]glucose, [3-^{13}C]sodium pyruvate and [2-^{13}C]glycerol were purchased from Omicron Biochemicals, Inc. (South Bend, IN). Other chemicals were of the highest purity available.

4.2. Preparation of [U–$^{13}C_5$]ribulose/ribose

A reaction mixture containing 100 mM Tris hydrochloride (pH 7.8), 6 mM dithiothreitol, 60 mM $MgCl_2$, 80 mM ATP, 200 mM ammonium acetate, 200 mM α-ketoglutarate, 5 mM $NADP^+$, 1 g of [U–$^{13}C_6$]glucose, 250 U of hexokinase, 250 U of glucose 6-phosphate dehydrogenase and 250 U of glutamate dehydrogenase in a total volume of 105 ml was incubated at 37°C. The pH of the solution was kept at pH 7.8 by adding of 3 M potassium hydroxide at intervals. The reaction was monitored by ^{13}C NMR spectroscopy. When the NMR signals of the intermediate, 6-phosphogluconate (C-1, 178.7 ppm; C-2, 74.1 ppm), had disappeared, 200 U of pentose isomerase were added, and the mixture was incubated for 2 h. To the resulting equilibrium mixture of [U–$^{13}C_5$]ribulose- and [U–$^{13}C_5$]ribose phosphate (2:1), 15 ml of 1 M barium chloride were added, and the suspension was centrifuged. The supernatant was diluted with 420 ml of ethanol and was kept at 4°C for 24 h. The precipitate of carbohydrate phosphate barium salts was harvested by centrifugation and redissolved in 100 ml of water. Six ml of 1 M $(NH_4)_2SO_4$ and 4 ml of 1 M K_2SO_4 were added and the precipitate of $BaSO_4$ was removed by centrifugation. The supernatant was concentrated at 35°C under reduced pressure to a small volume (80 ml). After addition of 2.5 ml of 100 mM $MgCl_2$ and 2.5 ml of 100 mM $ZnCl_2$, the pH value was adjusted to 7.9 with 1 M NaOH. Alkaline phosphatase (50 U) was added. The mixture was incubated at 37°C for 4 h and lyophilized.

The dry powder was dissolved in 40 ml of water, and the solution was applied on a column (2.2×43 cm) containing a mixture of 31.2 g of DOWEX

50W × 8 (H^+-form) and 42.9 g of DOWEX 1 × 8 (OH^--form). The column was developed with water. The effluent (450 ml) was collected, concentrated and lyophilized yielding 300 mg of a 2:1 mixture of [U–$^{13}C_5$]ribulose/ribose (total yield 37%).

4.3. Culture medium

Suspension cultures of *R. serpentina* were grown in LS medium (Linsmaier & Skoog, 1965) containing 1 μM 2,4-dichlorophenoxyacetic acid and 1 μM naphthylacetic acid. Alternatively, the cells were grown in AP medium (Zenk et al., 1977) containing 1 μM 3-indolylacetic acid, 5 μM N_6-benzyladenine and 20 mM $MgSO_4$. Sucrose was replaced by D-glucose in both culture media used (LS medium, 15 g D-glucose per liter; AP medium, 30 g D-glucose per liter, unless otherwise stated). The pH value of the media was adjusted to 6.0 with 0.1 M NaOH prior to sterilization.

4.4. Cell culture

Cells of *R. serpentina* were grown in 250-ml flasks containing 130 ml of LS medium. After 7 days of growth, 60 ml of cell suspension were added to 70 ml of LS medium. The cultures were incubated on a rotary shaker (130 rpm) at 21°C under a fluorescent tube (40 W, Duro Lite Inc., Midland Park, NJ).

For isotope incorporation experiments, 20 g of wet cell mass grown on LS medium for 7 days were suspended in 100 ml of modified AP-medium. ^{13}C-labeled nutrients were added as sterile solutions (Table 1). After a growth period of 18 days, the cells were harvested, frozen in liquid nitrogen and stored at −20°C.

4.5. High performance liquid chromatography

HPLC analysis of loganin was performed with a column of Nucleosil RP18 (4.55 × 250 mm) and an eluent containing 40 vol% methanol in water (flow rate, 1 ml/min). The effluent was monitored photometrically (254 nm). The retention volume of loganin was 9.5 ml.

4.6. Isolation of loganin

R. serpentina wet cell mass (100 g) was suspended in 50 ml of water and homogenized with an Ultra Turrax (10000 U/min, 5 min). The mixture was freeze-dried (3.5 g). Lyophilized plant material was extracted twice with 300 ml of methanol at room temperature for 24 h. The extracts were combined and concentrated under reduced pressure to a volume of 20 ml; 180 ml of water were added and insoluble material was removed by centrifugation (15 min, 7500 U/min, 4°C). The supernatant was applied on a column of Amberlite XAD-2 (2 × 10 cm). The column was washed with 250 ml of water. Loganin was eluted with 150 ml of methanol. The effluent was concentrated under reduced pressure to a volume of 10 ml.

Crude loganin was purified by preparative reversed-phase HPLC using a column of Nucleosil RP18 (16 × 250 mm). The column was developed with 40 vol% methanol (flow rate, 8 ml/min). The effluent was monitored photometrically (254 nm). The retention volume of loganin was 55 ml. Fractions containing loganin were combined and concentrated to dryness under reduced pressure.

4.7. Isolation of amino acids

Methanol-extracted cells were treated for 24 h at 120°C with 150 ml of 6 M HCl containing 0.5 M thioglycolic acid. The mixture was filtered and the supernatant was evaporated to dryness. Amino acids were isolated from the residue as described earlier (Eisenreich, Schwarzkopf, & Bacher, 1991).

4.8. NMR-spectroscopy

^1H and ^{13}C NMR spectra were recorded at 500 and 125 MHz, respectively, using a Bruker DRX 500 spectrometer. One- and two-dimensional experiments (DQF-COSY, NOESY, HMBC and INADEQUATE) were performed at 27°C using standard Bruker software (XWINNMR 1.3). Loganin was measured in D_2O as solvent. Amino acids were measured in D_2O at pH 1 or 13.

4.9. NMR signal assignment

The correct interpretation of ^{13}C labeling experiments by quantitative NMR spectroscopy requires unequivocal assignments of ^1H and ^{13}C NMR signals. NMR signals of loganin were assigned earlier on basis of chemical shift arguments (Heckendorf, Mattes, Hutchinson, Hagaman, & Wenkert, 1976; Jensen, Lyse-Petersen, & Nielsen, 1979; Calis, Lahloub, & Sticher, 1984). In order to obtain unequivocal NMR signals assignments, we performed a comprehensive NMR analysis by two-dimensional homo- and hetero-correlation experiments (Table 4). The $^{13}C^{13}C$ coupling patterns of loganin from the incorporation experiment with [U–$^{13}C_6$]glucose and [U–$^{13}C_5$]ribulose/ribose gave additional confirmation of the ^{13}C NMR assignments via INADEQUATE experiments.

4.10. Quantitative analysis of ^{13}C labeling patterns

Absolute ^{13}C abundance was determined for each carbon atom of loganin from the feeding experiments

Table 4
Assignments of the ^{1}H and ^{13}C NMR signals of loganin

Position	Chemical shifts		Coupling constants		DQF-COSY	NOESY[c]	HMBC[d]	INADEQUATE[e]
	^{13}CC (ppm)	^{1}H (ppm)	J_{CC}[b] (Hz)	J_{HH} (Hz)				
11	170.0(C)[a]		77.9(4)				3, 12	4
3	150.8(CH)	7.30	76.8(4)			5, 7, 10(w), 4′(w), 2′(w), 3′ or 5′(w), 6′a(w)	1, 5	4
4	113.0(C)		76.9(3), 77.9(11), 44.1(5)				3, 5, 6a, 6b, 9	3, 11
1′	98.5(CH)	4.66(d)	46.5(2′), 5.2(3′)	7.8(2′)	2′	2′, 4′(w), 3′ or 5′(s)	1, 2′	1′, 2′, 3′
1	96.6(CH)	5.27(d)	43.5(9), 4.15(7)	3.6(9)	9	7, 8, 9 (s), 10	1′, 3, 5, 8, 9	7, 9
5′	76.2(CH)	3.35–3.41(m)	41.0(4′), 43.1(6′)	2.2(6′a), 6.1(6′b)	6′a, 6′b	ND[f]		4′, 6′
3′	75.6(CH)	3.35–3.41(m)	39.0(2′), 40.0(4′)		2′, 4′	ND[f]		1′, 2′, 4′
7	74.2(CH)	4.01(t)	36.6(8)	5.6(6a)[g], 5.6(8)[g]	6a, 6b(w), 8	1, 3, 6a, 8(s), 10(w)	5, 6a, 6b	1, 9
2′	72.6(CH)	3.17(t)	47.0(1′), 39.0(3′)	8.1(1′, 3′)	1′, 3′	1′, 3′(w)		1′, 3′
4′	69.5(CH)	3.29	40.0(3′), 41.0(5′)		3′, 5′	1′(w), 3(w), 6′a	2′, 6′a, 6′b	3′, 5′
6′a	60.6(CH_2)	3.81(dd)	43.1(5′)	2.2(5′), 12.4(6′b)	5′, 6′b	3(w), 4′, 3′ or 5′, 6′b or 12	4′	5′
6′b	60.6(CH_2)	3.61(dd)	43.1(5′)	6.1(5′), 12.4(6′a)	5′, 6′a	ND[f]		
12	51.7(CH_3)	3.62(s)				ND[f]		
9	44.8(CH)	2.0(m)	43.4(1), 31.3(5), 33.9(8)	3.6(1), 8.5(5)[g], 9.4(8)[g]	1, 5, 8	1(s), 5(s), 10(s)	5, 6a, 6b, 7, 8, 10	1, 7
6a	40.2(CH_2)	1.60(m)	33.3(5)	6.8(5)[g], 14.7(6b)[g], 5.6(7)[g]	5, 6b, 7	6b(s), 7		5
6b	40.2(CH_2)	2.06(m)	33.3(5)	7.9(5), 14.6(6a)[g]	5, 6a, 7	5, 6a(s)		5
8	40.0(CH)	1.77(m)	36.7(10), 33.3(9)	9.4(9)[g], 6.9(10), 5.6(7)[g]	7, 9, 10	1, 7(s), 10(s)		10
5	29.7(CH)	2.95(q)	33.2(6), 31.3(9), 44.1(4)	7.9(6a, 6b)[g], 8.5(9)[g]	6a, 6b, 9	3, 6b, 9(s)	1, 3, 6a, 6b, 7, 9	6
10	11.9(CH_3)	0.95(d)	36.3(8)	6.9(8)	8	1, 7(w), 8(s), 9(s)		8

[a] Determined by DEPT analysis.
[b] $^{13}C^{13}C$ coupling constants obtained from one-dimensional proton-decoupled ^{13}C NMR spectra of biosynthetically enriched samples. Carbons coupled to the respective index carbon are in parentheses.
[c] Mixing time, 2 s.
[d] Observed proton correlations to the respective index carbon atoms.
[e] Optimized for small coupling constants. Performed with a sample from the incorporation experiment with [U–$13C_6$]glucose.
[f] ND, not determined due to signal overlap.
[g] Coupling constants obtained by simulation with NMRSIM (Bruker).

by quantitative NMR spectroscopy (Strauß, Eisenreich, Bacher, & Fuchs, 1992). Briefly, ^{1}H decoupled ^{13}C NMR spectra of the biosynthetic samples and of samples with natural ^{13}C abundance (1.1% ^{13}C) were measured under identical conditions. This standardization considers different relaxation behavior of carbon atoms and prevents false quantification of ^{13}C abundances due to differences in relaxations times. Relative ^{13}C abundance of individual carbon atoms was then calculated from the integrals of biosynthetic samples by comparison with the natural abundance samples. In order to obtain absolute ^{13}C abundances, the ^{13}C satellites in the ^{1}H NMR of each metabolite were analyzed yielding absolute ^{13}C abundance values for selected carbon atoms. The relative abundances were subsequently referenced to these respective carbon atoms (Eisenreich, Sagner, Zenk, & Bacher, 1997).

4.11. Analysis of isotopomer composition

The fraction of multiply labeled isotopomers was calculated from ^{1}H-decoupled ^{13}C NMR spectra as the fraction of $^{13}C^{13}C$ coupled satellites in the global ^{13}C NMR integral of the respective carbon atom. Multiplication with the absolute ^{13}C abundance value of the corresponding position yielded the fraction of multiply labeled isotopomers in mol%.

4.12. NMR spectra simulation

^{1}H- and ^{13}C-coupling patterns were simulated with the program package NMRSIM (Bruker).

Acknowledgements

This work was supported by the Deutsche Forschungsgemeinschaft (SFB 369) and the Fonds der chemischen Industrie. We thank Professor Duilio Arigoni for many helpful discussions and Angelika Werner and Fritz Wendling for help with the preparation of the manuscript.

References

Arigoni, D., Sagner, S., Latzel, C., Eisenreich, W., Bacher, A., & Zenk, M. H. (1997). *Proc. Natl. Acad. Sci. USA*, *94,* 10600–10605.

Bacher, A., Rieder, C., Eichinger, D., Arigoni, D., Fuchs, G., & Eisenreich, W. (1998). *FEMS Microbiol. Rev.*, in press.

Banthorpe, D. V., Charlwood, B. V., & Francis, M. J. O. (1972). *Chem. Rev.*, *72,* 115–155.

Battersby, A. R., Burnett, A. R., Parsons, P. G. (1969). *J. Chem. Soc. (C)*, 1187–1192.

Battersby, A. R., Byrne, J. C., Kapil, R. S., Martin, J. A., Payne, T. G., Arigoni, D., Loew, P. (1968). *J. Chem. Soc. Chem. Commun.*, 951–953.

Bloch, K. (1992). *Steroids*, *57,* 378–382.

Brechbühler-Bader, S., Coscia, C. J., Loew, P., v. Sczepanski, C., Arigoni, D. (1968). *J. Chem. Soc. Chem. Commun.*, 136–137.

Broers, S. T. J. (1994). Thesis No. 10978, ETH Zürich, Switzerland.

Calis, I., Lahloub, M. F., & Sticher, O. (1984). *Helv. Chim. Acta*, *67,* 160–165.

Campos, N., Lois, L. M., & Boronat, A. (1997). *Plant Physiol.*, *115,* 1289.

Disch, A., Schwender, J., Müller, C., Lichtenthaler, H. K., & Rohmer, M. (1998). *Biochem. J.*, *333,* 381–388.

Eisenreich, W., Sagner, S., Zenk, M. H., & Bacher, A. (1997). *Tetrahedron Lett.*, *38,* 3889–3892.

Eisenreich, W., Schwarz, M., Cartayrade, A., Arigoni, D., Zenk, M. H., & Bacher, A. (1998). *Chem. Biol.*, *5,* 221–233.

Eisenreich, W., Schwarzkopf, B., & Bacher, A. (1991). *J. Biol. Chem.*, *266,* 9622–9631.

Escher, S., Loew, P., Arigoni, D. (1970). *J. Chem. Soc. Chem. Commun.*, 823–825.

Flesch, G., & Rohmer, M. (1988). *Eur. J. Biochem.*, *175,* 405–411.

Guarnaccia, R., Botta, L., & Coscia, C. J. (1974). *J. Am. Chem. Soc.*, *96,* 7079–7084.

Heckendorf, A. H., Mattes, K. C., Hutchinson, C. R., Hagaman, E. W., & Wenkert, E. (1976). *J. Org. Chem.*, *41,* 2045–2047.

Jensen, S. R., Lyse-Petersen, S. E., & Nielsen, B. J. (1979). *Phytochemistry*, *88,* 273–277.

Lange, B. M., Wildung, M. R., McCaskill, M. R., & Croteau, D. (1998). *Proc. Natl. Acad. Sci. USA*, *95,* 2100–2104.

Linsmaier, E. M., & Skoog, F. (1965). *Physiol. Plant.*, *18,* 100–127.

Lois, L. M., Campos, N., Putra, S. R., Danielsen, K., Rohmer, M., & Boronat, A. (1998). *Proc. Natl. Acad. Sci. USA*, *95,* 2105–2110.

Menhard, B. (1998). Biosynthesis of taxans and their elicitation. International Symposium Antitumor Products from Higher Plants, Paris, January 8–10, 1998.

Qureshi, N., & Porter, J. W. (1981). In: J. W. Porter, & S. L. Spurgeon. *Biosynthesis of isoprenoid compounds*, (Vol. 1, pp. 47–94). New York: John Wiley.

Ramos-Valdivia, A., van der Heijden, R., & Verpoorte, R. (1997). *Nat. Prod. Rep.*, *14,* 591–603.

Rohmer, M. (1998). *Prog. Drug. Res.*, *50,* 135–154.

Rohmer, M., Knani, M., Simonin, P., Sutter, B., & Sahm, H. (1993). *Biochem. J.*, *295,* 517–524.

Sagner, S., Eisenreich, W., Fellermeier, M., Latzel, C., Bacher, A., & Zenk, M. H. (1998). *Tetrahedron Lett.*, *39,* 2091–2094.

Schwarz, M. K. (1994). Thesis No. 10951, ETH Zürich, Switzerland.

Schwender, J., Lichtenthaler, H. K., et al. (1997). *FEBS Lett.*, *414,* 129–134.

Shanks, J. V., Bhadra, R., Morgan, J., & Rijhwani, S. (1998). *Biotechnol. Bioeng.*, *58,* 333–338.

Sprenger, G. A., Sahm, H., et al. (1997). *Proc. Natl. Acad. Sci. USA*, *94,* 12857–12862.

Stöckigt, J. (1979). *Habilitation*. Germany: Ruhruniversität Bochum.

Strauß, G., Eisenreich, W., Bacher, A., & Fuchs, G. (1992). *Eur. J. Biochem.*, *205,* 853–866.

Takahashi, S., Kuzuyama, T., Watanabe, H., & Seto, H. (1998). *Proc. Natl. Acad. Sci. USA*, *95,* 9879–9884.

Tanahashi, T., Nagakura, N., Inouye, H., & Zenk, M. H. (1984). *Phytochemistry*, *23,* 1917–1922.

Uesato, S., Kanomi, S., Iida, A., Inouye, H., & Zenk, M. H. (1986). *Phytochemistry*, *25,* 839–842.

Verpoorte, R., van der Heijden, R., & Moreno, P. R. H. (1997). In: G. A. Cordell. *The alkaloids* (Vol. 49, pp. 221–299). New York: Academic Press.

Werner, I., Bacher, A., & Eisenreich, W. (1997). *J. Biol. Chem*., *272,* 25474–25482.

Whitmer, S., Canel, C., Hallard, D., Gonçalves, C., & Verpoorte, R. (1998). *Plant Physiol*., *116,* 853–857.

Zenk, M. H., El-Shagi Arens, H., Stöckigt, J., Weiler, E. W., & Deus, B. (1977). In: W. Barz, E. Reinhard, & M. H. Zenk. Plant tissue culture and its biotechnological application (pp. 27). Berlin: Springer.